JOURNAL OF NANO- AND ELECTRONIC PHYSICS
Vol. **17** No 4, 04019(5pp) (2025)

ЖУРНАЛ НАНО- ТА ЕЛЕКТРОННОЇ ФІЗИКИ
Том **17** № 4, 04019(5cc) (2025)

OPEN ACCESS

REGULAR ARTICLE

Highly-Isolated Compact Quad-Lobed UWB MIMO Antenna with Hexagonal Slot for Enhanced 5G and Industrial IoT Applications

Bappadittya Roy[1,*], Hemalatha T[2,†]

[1] *School of Electronics Engineering, VIT – AP University, 522237 Inavolu, Amaravati, India*
[2] *Vijaya Institute of Technology for Women, 521108 Enikepadu, India*

(Received 07 April 2025; revised manuscript received 18 August 2025; published online 29 August 2025)

A compact Quad-Lobed Hexagonal Ring Slotted Ultra-Wideband (UWB) Multiple-Input Multiple-Output (MIMO antenna), featuring dimensions of $1.68\lambda_0 \times 1.68\lambda_0 \times 0.0675\lambda_0$, is proposed to address the critical challenges associated with improving isolation in MIMO antennas. A Mutual Coupling Reduction Ring (MCRR) is introduced to improve the high isolation among the radiating elements. The design employs innovative techniques, including the use of hexagonal ring slots, to achieve an extended impedance bandwidth of 17.1 GHz. Key performance metrics such as a reflection coefficient (S11 < – 10 dB), isolation (S21 < – 20 dB), and diversity parameters have been thoroughly evaluated. The antenna demonstrates exceptional performance, including a maximum |S11| of 44.7 dB at 9.6 GHz, a peak gain of 9.5 dBi, ECC < 0.0025, TARC < – 10 dB, and a diversity gain around 10 dB. The wide impedance bandwidth and compact form factor make this design versatile for integration into modern communication systems, such as vehicular communication systems, smart healthcare equipment, ensuring reliable and high-speed data transmission. Additionally, the antenna's simple structure and efficient design minimize fabrication complexity, making it a cost-effective solution for modern wireless systems. Its adaptability across multiple frequency bands ensures seamless operation in sensor networks and autonomous systems.

Keywords: Isolation, UWB, MIMO, Hexagonal slot, 5G, IoT.

DOI: 10.21272/jnep.17(4).04019 PACS numbers: 84.40.Ba

1. INTRODUCTION

Ultra-Wideband (UWB) Multiple-Input Multiple-Output (MIMO) technology represents a cutting-edge advancement in wireless communication systems. This sophisticated technology utilizes multiple antennas at both the transmitting and receiving ends to enhance data transmission rates, improve reliability, and mitigate multipath fading effects. The use of UWB enables high data rates suitable for applications such as high-definition multimedia streaming, precise indoor positioning, and robust wireless sensor networks [1]. Recent advancements, such as the MIMO circular patch microstrip antenna (CPMA) operating at 3.5 GHz and 6 GHz [2], and a semicircular monopole patch with innovative slotting for improved impedance matching and bandwidth [3], have demonstrated significant performance improvements. However, despite these advancements, challenges remain in achieving high isolation and bandwidth efficiency without introducing excessive design complexity or cost. Existing isolation enhancement techniques, including Split Ring Resonators [4], Metamaterial superstrates [5], Frequency Selective Surfaces (FSS) [6], and Electromagnetic Band Gaps (EBG) [7, 8], often lead to increased design complexity and higher manufacturing costs. Additionally, while methods such as Complementary Split Ring Resonators (CSRR) [9], Defected Ground Structures (DGS) [11], and self-isolation techniques [12, 13] improve isolation, integrating these solutions into compact and efficient MIMO antenna designs remains challenging. Many current designs are optimized for specific frequency bands, limiting their applicability to wideband or UWB systems. To address these limitations, this study proposes a novel Quad-lobed Hexagonal Slotted MIMO antenna that achieves high isolation and bandwidth efficiency while maintaining a compact and cost-effective design. The objectives of this research are to develop a MIMO antenna with superior isolation performance (> 20 dB) suitable for UWB applications, minimize mutual coupling effects through innovative MCRR, achieve wideband operation while maintaining compact dimensions, and ensure ease of fabrication for practical applications. By addressing these objectives, this work aims to bridge existing research gaps and provide an efficient, high-performance solution for real-world applications such as 5G systems, high-speed data transmission, and precise positioning systems.

2. DESIGN STAGES OF THE PROPOSED ANTENNA DESIGN

The proposed four-port lobed antenna design occupies

* Correspondence e-mail: bappadittya.roy@vitap.ac.in
† hemanaeem2299@gmail.com

© 2025 The Author(s). Journal of Nano- and Electronic Physics published by Sumy State University. This article is distributed under the terms and conditions of the Creative Commons Attribution (CC BY) license.

Cite this article as: B. Roy et al., *J. Nano- Electron. Phys.* 17 No 4, 04019 (2025) https://doi.org/10.21272/jnep.17(4).04019

a total physical volume of $1.68\lambda_0 \times 1.68\lambda_0 \times 0.0675\lambda_0$ mm^3 and is implemented on FR4_epoxy substrate with a ε_r of 4.4, 1.6 mm thickness and a loss tangent of 0.02. The progression of the proposed antenna design is explained in this section.

Stage 1: Baseline Antenna Design (Antenna-1)

The initial design involves the development of four oval-shaped patch antennas, each characterized by distinct major and minor radii, denoted as R1 and R2, respectively. These patch elements are positioned orthogonally to form a compact antenna array configuration. The design incorporates a partial ground plane to achieve a balanced performance across various parameters. This initial structure is referred to as Antenna-1 and is illustrated in Fig. 1(a).

Stage 2: Incorporation of Hexagonal ring slot (Antenna-2)

The incorporation of a hexagonal ring slot into the patch significantly enhances the antenna's bandwidth from 7.2 GHz to 11.4 GHz, resulting in an overall frequency range from 6.1 GHz to 17.5 GHz. This improvement is attributed to the hexagonal slot's ability to modify the current distribution on the patch surface, enhancing impedance matching across a broader frequency range.

Stage 3: Partial Ground Stub Slot (Antenna-3)

In the third iteration, a stub slot is introduced on the partial ground plane to further improve the bandwidth and the MIMO antenna's gain. The addition of this stub effectively refines the impedance matching and boosts the overall radiation efficiency. This iteration is referred to as Antenna-3 and is shown in Fig. 1(c).

Stage 4: Integration of Mutual Coupling Reduction Ring (Antenna-4)

The final stage involves the placement of a Mutual Coupling Reduction Ring (MCRR) between the individual antenna elements to minimize interference and enhance isolation. This isolation structure significantly reduces mutual coupling effects, thereby improving the effectiveness of the MIMO antenna with respect to signal clarity and efficiency. The final optimized design is termed as the Proposed design (Antenna-4) and is presented in Fig. 1(d).

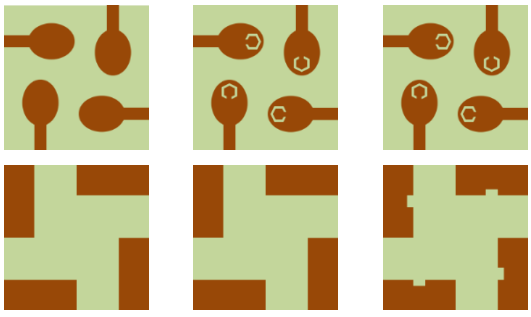

(a) Antenna – 1 (b) Antenna – 2 (c) Antenna – 3

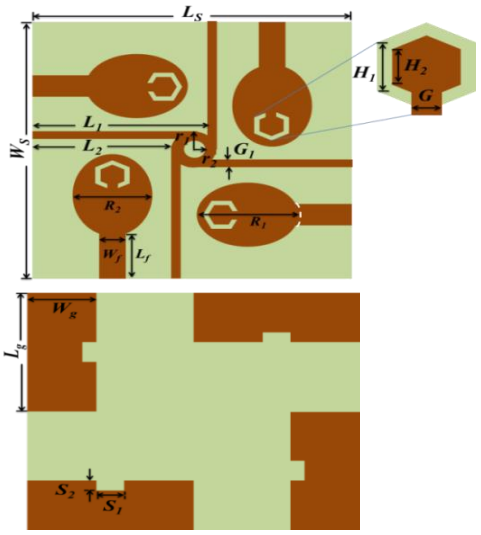

(d) Antenna – 4 (Proposed structure)

Fig. 1 – Design evolution of Quad-Lobed MIMO

Table 1 – Dimensions of the hexagonal slotted quad-lobed MIMO antenna (in mm)

Variables	Measurements (mm)	Variables	Measurements (mm)
L_s	40	S_2	1.5
W_s	40	H_1	2.5
L_g	20	H_2	1.5
W_g	6	G	1
R_1	13	L_1	21.5
R_2	10.4	L_2	17.4
L_f	6.77	G_1	1.5
W_f	3	r_1	3
S_1	3	r_2	1.5

The proposed antenna design's dimensions are outlined in Table 1. The proposed structure was designed using HFSS R2 2020, and the corresponding simulation results are elaborated in Section 3.

3. RESULTS AND DISCUSSION

Figure 2 illustrates the reflection coefficients at different levels of design evolution. Antenna-1, featuring quad-lobed patches arranged orthogonally with a partial ground plane, achieved two bandwidths. The first bandwidth spans 6.2 GHz to 9.4 GHz, resulting in an achieved bandwidth of 3.2 GHz, and the second bandwidth extends from 11.5 to 18.7 GHz, corresponding to an achieved bandwidth of 7.2 GHz. The reflection coefficients for these bandwidths are – 32.51 dB at 8.2 GHz and – 27.55 dB at 15.1 GHz, respectively.

The incorporation of a hexagonal ring slot into the patch significantly enhanced the antenna's bandwidth. The achieved bandwidth increases from 7.2 GHz to 11.4 GHz, resulting in an overall frequency range from 6.1 GHz to 17.5 GHz. This improvement is attributed to the hexagonal slot's ability to modify the current distribution on the patch surface, enhancing impedance matching across a broader frequency range. The reflection coefficient for this configuration is recorded at – 28.19 dB at 15.1 GHz, indicating improved signal

efficiency. A stub slot on the partial ground plane is introduced to further enhance the antenna's bandwidth. The achieved bandwidth increases from 11.4 GHz to 16.7 GHz (4.3 GHz-21.0 GHz). The stub slot acts as a reactive element, optimizing impedance matching and improving resonance characteristics. At this stage, the reflection coefficient improves to – 30.74 dB at 14.4 GHz. Additionally, mutual coupling between adjacent antenna elements becomes more prominent, achieving an isolation level of < 15 dB.

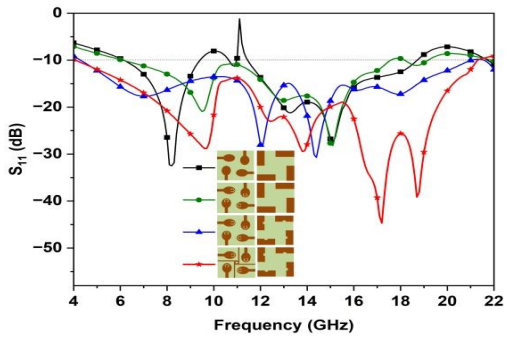

Fig. 2 – Reflection Coefficient at various stages of design evolution

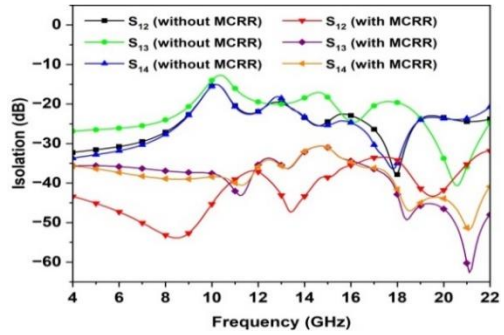

Fig. 3 – Isolation between the MIMO antenna elements

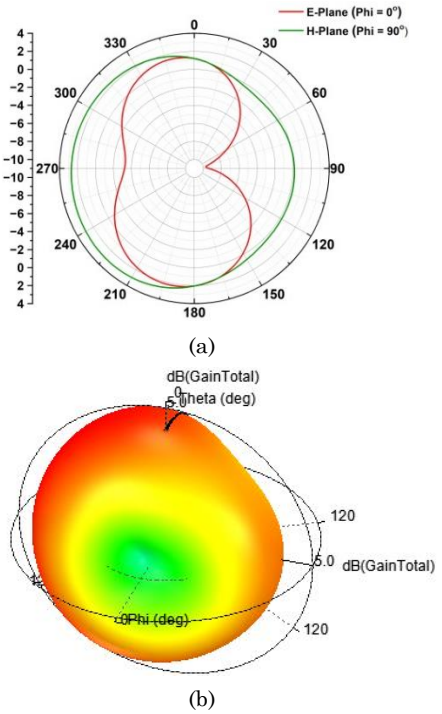

Fig. 4 – Far-field radiation patterns at 9.6 GHz (a) 2D (b) 3D

The stub also helps suppress unwanted surface currents, contributing to better radiation performance. An MCRR incorporated between the radiating elements disrupts surface wave propagation by introducing a resonant structure that mitigates coupling between adjacent elements. As a result, the achieved bandwidth extends from 16.7 GHz to 17.1 GHz, covering a range from 4.1 GHz to 21.2 GHz. The reflection coefficient shows a optimum refinement of – 44.7 dB at 17.1 GHz, indicating superior impedance matching and lower return loss. The MCRR integration also significantly enhances the isolation between antenna elements, increasing from 15 dB to greater than 40 dB in the final design, depicted in Fig. 3. This improvement in isolation is critical for MIMO systems, as it reduces interference between elements and enhances overall system performance.

Figure 4 illustrates the radiation pattern of the antenna, displaying its performance in both the *E*-plane (Φ = 0°) and the *H*-plane (Φ = 90°). The *E*-plane demonstrates bidirectional radiation with higher directivity along the broadside direction.

In contrast, the *H*-plane shows a more omnidirectional pattern, providing uniform radiation across a wider angle. The *E*-plane focuses energy in specific directions, while the *H*-plane ensures broader coverage, makes the antenna suitable for broadband MIMO applications. Figures 5(a), 5(b) illustrates the distribution of surface current of a quad-element MIMO system with and without MCRR when port 1 is excited. In Fig. 5(a), it is evident that the surface currents spreading across the feedlines and neighboring elements, signifying weaker isolation and higher mutual coupling, which suggests the requirement of isolation mechanism. In Fig. 5(b), the surface currents are predominantly confined to the radiating patches and their immediate surroundings, indicating effective suppression of mutual coupling between the elements, which indicates the effective cancellation of coupled currents and enhanced the isolation between the neighbor elements.

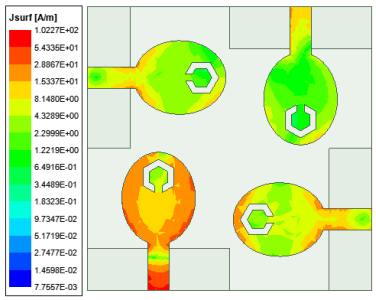

(a) Without MCRR

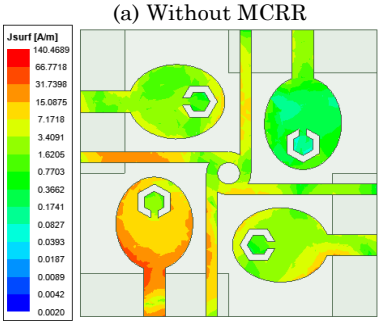

(b) With MCRR

Fig. 5 – Surface current distribution at 9.6 GHz

In MIMO systems, three critical metrics associated with diversity performance are the ECC, TARC, and Diversity Gain (DG). The correlation coefficient measures the level of correlation or independence between multipath communication channels. The ECC can be evaluated using far-field radiation patterns through equation (1) [13]. An ECC value of < 0.0025 was obtained, as shown in Fig. 6(a).

$$ECC = \frac{\left|\iint_{4\pi}[E_i(\theta,\phi) \times E_j(\theta,\phi)]d\Omega\right|^2}{\iint_{4\pi}|E_i(\theta,\phi)|^2 d\Omega \times \iint_{4\pi}|E_j(\theta,\phi)|^2 d\Omega} \quad (1)$$

The TARC value remains below -10 dB, demonstrating excellent isolation between the radiating elements, depicted in Fig. 6(b). Additionally, a diversity gain of approximately 10 dB was achieved, calculated using equation (2) [13], shown in Fig. 7(a).

$$DG = 10\sqrt{1-(ECC)^2} \quad (2)$$

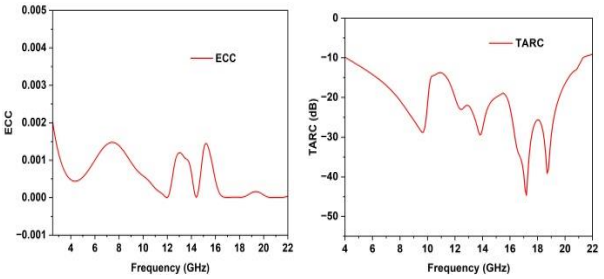

(a) (b)

Fig. 6 – (a) ECC (b) TARC

The peak gain remains relatively stable at lower frequencies, averaging around 2-4 dB. However, a significant increase is observed near 16.5 GHz, where the gain reaches its maximum value of approximately 9.5 dBi, shown in Fig. 7(b).

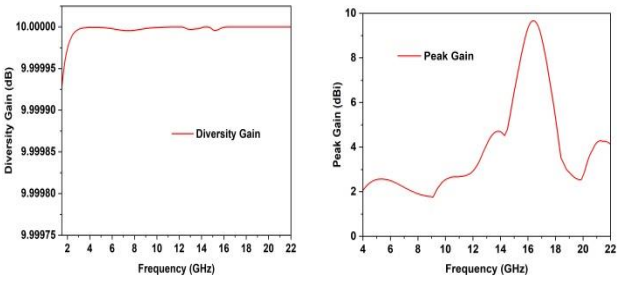

(a) (b)

Fig. 7 – (a) Diversity gain (b) Peak gain (dBi)

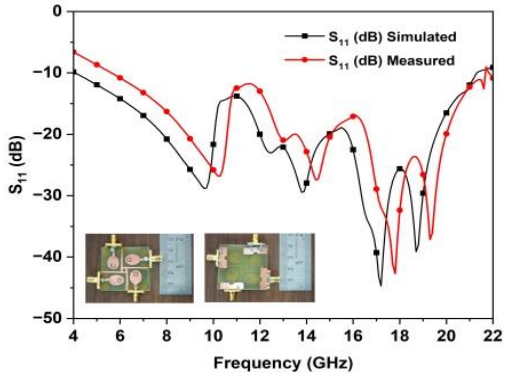

Fig. 8 – Sim. vs. Mea. – Reflection Coefficient

The comparative results show strong agreement, with minor deviations attributed to fabrication imperfections and measurement losses, as illustrated in Fig. 8 along with the embedded images of the fabricated antenna prototype.

Table 2 – Performance assessment of the Quad-Lobed MIMO design with traditional antenna designs

Ref. No	Dimensions (mm^2)	Frequency Range (GHz)	Bandwidth (GHz)	S11 (dB)	Peak gain (dBi)	ECC	No. of antenna elements	Isolation (dB)
[8]	$1.64\lambda_0 \times 1.40\lambda_0$	1.7 – 12.4	10.7	– 25	5.78	< 0.05	4	> 15
[9]	$0.63\lambda_0 \times 0.63\lambda_0$	2.08 – 2.25	0.17	– 25	6.28	< 0.00008	4	> 13
[12]	$4.30\lambda_0 \times 2.58\lambda_0$	23.8 – 27.5	3.7	– 40	6.5	–	2	–
[13]	$1.90\lambda_0 \times 1.90\lambda_0$	5.06-19.34	14.28	– 40	10.6	< 0.0044	4	> 20
[14]	$0.63\lambda_0 \times 0.63\lambda_0$	2.9 – 11.6	8.7	– 20	7	< 0.02	2	> 16
This work	$1.68\lambda_0 \times 1.68\lambda_0$	4.1 – 21.2	17.1	– 44.7	9.5	< 0.0025	4	> 40

4. CONCLUSION

The proposed Quad-Lobed Hexagonal Ring Slotted UWB MIMO antenna, with its compact design and innovative features such as the MCRR, effectively addressed the challenges of isolation in MIMO antenna systems. The antenna achieved high performance across key metrics, including extended impedance bandwidth, superior reflection coefficient, high isolation and low ECC, making it highly suitable for diverse applications.

The MIMO antenna ability to deliver reliable and high-speed data transmission, combined with a cost-effective and fabrication-friendly design, highlights its potential for integration into advanced 5G wireless systems and various IoT based industrial applications. Furthermore, the antenna's high peak gain and low TARC values contribute to efficient signal transmission, making it a robust solution for next-generation wireless communication systems.

ACKNOWLEDGEMENT

The authors extend their gratitude to the Department of SENSE at VIT-AP University, RGEMS, V-Launch Projects and Department of ECE, VITW for their invaluable provision and inspiration during the course of this research endeavor.

REFERENCES

1. N.H. Jemaludin, Nazrin Haziq Bin, et al., *Res. Eng.* **23**, 102712 (2024).
2. Surjati, Indra, et. al., *J. Nano- Electron. Phys.* **16** No 2, 02009 (2024).
3. Praveen Kumar, et al., *IEEE Trans. Circ. Syst. II: Exp. Briefs* **70** No 3, 949 (2022).
4. M. Li, X. Chen, A. Zhang, W. Fan, A.A. Kishk, *IEEE Antennas Wireless Propag. Lett.* **19** No 10, 1828 (2020).
5. L. Si, H. Jiang, X. Lv, J. Ding, *Opt. Express* **27** No 3, 3472 (2019).
6. Tayyab Hassan, et. al., *IEEE Trans. Antennas Propag.* **66** No 9, 4900 (2018).
7. H. T, B. Roy, *IEEE Open J. Antennas Propag.* **5** No 3, 634 (2024).
8. D. Kumutha, et al., *J. Nano- Electron. Phys.* **16** No 6, 06015 (2024).
9. B. Sivashanmugavalli, B. Vijayalakshmi, *J. Nano-Electron. Phys.* **16** No 5, 05012 (2024).
10. Z. Zhou, Y. Ge, J. Yuan, Z. Xu, Z.D. Chen, *IEEE Trans. Antennas Propag.* **71** No 2, 1414 (2023).
11. B. Qian, X. Chen, A. Kishk, *IEEE Antennas Wireless Propag. Lett.* **20** No 5, 828 (2021).
12. N. Meskini, et al., *J. Nano- Electron. Phys.* **16** No 3, 03006 (2024).
13. H. T, B. Roy, *J. Nano- Electron. Phys.* **16** No 4, 04010 (2024).
14. Z. Li, C. Yin, X. Zhu, *IEEE Access* **7**, 38696 (2019).

Високоізольована компактна чотирипелюсткова UWB MIMO-антена з шестигранним слотом для розширених застосувань 5G та промислового інтернету речей

Bappadittya Roy[1], Hemalatha T[2]

[1] *School of Electronics Engineering, VIT – AP University, 522237 Inavolu, Amaravati, India*
[2] *Vijaya Institute of Technology for Women, 521108 Enikepadu, India*

Для вирішення критичних проблем, пов'язаних з покращенням ізоляції в MIMO-антенах, пропонується компактна чотирипелюсткова шестигранна кільцева щілинна надширокосмугова (UWB) антена з кількома входами та кількома виходами (MIMO) розмірами $1{,}68\lambda_0 \times 1{,}68\lambda_0 \times 0{,}0675\lambda_0$. Для покращення ізоляції між випромінюючими елементами впроваджено кільце взаємної редукції зв'язку (MCRR). У конструкції використовуються інноваційні методи, включаючи використання шестигранних кільцевих щілин, для досягнення розширеної смуги пропускання імпедансу 17,1 ГГц. Були оцінені ключові показники продуктивності, такі як коефіцієнт відбиття (S11 = – 10 дБ), ізоляція (S21 = – 20 дБ) та параметри рознесення. Антена демонструє виняткову продуктивність, включаючи максимальну |S11| 44,7 дБ на частоті 9,6 ГГц, пікове посилення 9,5 дБі, ECC < 0,0025, TARC < –10 дБ та посилення рознесення близько 10 дБ. Широка смуга пропускання імпедансу та компактний форм-фактор роблять цю конструкцію універсальною для інтеграції в сучасні системи зв'язку, такі як системи автомобільного зв'язку, інтелектуальне медичне обладнання, забезпечуючи надійну та високошвидкісну передачу даних. Крім того, проста структура та ефективний дизайн антени мінімізують складність виготовлення, що робить її економічно ефективним рішенням для сучасних бездротових систем. Її адаптивність до кількох діапазонів частот забезпечує безперебійну роботу в сенсорних мережах та автономних системах.

Ключові слова: Ізоляція, UWB, MIMO, Шестикутний слот, 5G, Інтернет речей.